An energy management of a combined cooling and power cogeneration system using hydrogen energy for an off-grid application

Hugo Lambert, Franco Ferrucci, Robin Roche, Samir Jemei, Pascal Ortega, Daniel Hissel

An energy management of a combined cooling and power cogeneration system using hydrogen energy for an off-grid application

Hugo Lambert
FEMTO-ST Institute
Univ. Bourgogne Franche-Comté, CNRS
Belfort, France
hugo.lambert@femto-st.fr

Franco Ferrucci
GEPASUD
Univ. de la Polynésie française
Faa'a, French Polynesia
franco.ferrucci@upf.pf

Robin Roche
FEMTO-ST Institute
UTBM, Univ. Bourgogne Franche-Comté, CNRS
Belfort, France
robin.roche@utbm.fr

Samir Jemeï
FEMTO-ST Institute
Univ. Bourgogne Franche-Comté, CNRS
Belfort, France
samir.jemei@univ-fcomte.fr

Pascal Ortega
GEPASUD
Univ. de la Polynésie francaise
Faa'a, French Polynesia
pascal.ortega@upf.pf

Daniel Hissel
FEMTO-ST Institute
Univ. Bourgogne Franche-Comté, CNRS
Belfort, France
daniel.hissel@univ-fcomte.fr

***Abstract*—In order to decarbonize electricity production in insular tropical regions, hydrogen as an energy vector appears to be a promising solution. But some issues have to be dealt with, like the overall yield of the hydrogen chain. Moreover, thermochemical systems can produce cooling by thermal recovery. In this paper, we study a system composed by an electrolyzer, a hydrogen fuel cell, a Li-ion battery pack and a thermochemical reactor coupled with a conventional ammonia heat pump. In this system, the waste-heat from the electrolyzer and the fuel cell are used to desorb a thermochemical reactor for a differed production of cooling. A Mixed Integer Linear Program is used to optimize the energy management, taking into account the electrical and thermal load demand and the aging of the electrolyzer, the fuel cell and the battery. Results show that the system is able to provide the electrical and thermal needs of the load and the use of the thermochemical cooling system improves the fuel cell and the electrolyzer efficiency by 21% and 15% respectively compared to a system without thermochemical storage.**

***Index Terms*—energy management, hydrogen energy, MILP, combined cooling and power, cogeneration, off-grid, fuel cell, electrolyzer, thermochemical storage**

I. Introduction

French Polynesia is composed of hundreds of small islands spread out over an area bigger that the European Union. French Polynesia is also extremely dependent to oil importations as 93% of the final energy comes from hydrocarbons [1]. Tropical areas are characterized by warm temperatures all along the year where air conditioning represents a large part of the electrical consumption in the residential sector. In order to decarbonize electricity and cooling production, a hybrid system combining PV panels with a hydrogen storage system and a battery storage for electricity storage and production, and a heat pump with a thermochemical reactor for cooling production and storage, is used in this paper. Hydrogen storage systems combine an electrolyzer for the hydrogen production, a tank for hydrogen storage and a fuel cell for the electricity production using the hydrogen stored. In [2], authors made a review covering the integration of hydrogen systems into power system and [3] describes how fuel cell systems are used for cogeneration and tri-generation systems. A rule-based strategy in [4], has been applied to provide electrical need of an isolated load. They used a fuel cell and a diesel generator as backup power units. Using hydrogen storage system in their application reduced by 97.8% the CO_2 emissions compared to the diesel backup generator. In [5], authors used a particle swarm optimization algorithm to minimize the component sizing of a stand-alone electrical load. They proved that hydrogen storage reduces the sizing of PV panels and battery capacity and also that renewable energy based solution is cheaper than diesel based system. Our previous work [6] uses a rule-based energy management in order to provide electrical and cooling needs in an isolated application. But, without the optimization process, a part of the energy provided by the PV panels were lost and the aging of components was not taken into account.

As the fuel cell and the electrolyzer produce heat during their process, this heat can be recovered and thus improves the fuel efficiency and the hydrogen storage system overall efficiency. With respect to waste-heat recovery methods applied to hydrogen based installations, [7] reviews the thermal recovery opportunity of low temperature fuel cells and presents the sorption method for cooling generation. Sorption systems are used in order to recover the heat of process and convert this heat into cooling energy as a heat pump [8], [9], [10]. This gives the opportunity to emissions reduction and energy efficiency improvement. The work in [11], has been used as a reference for the thermochemical cooling system (TCS) modeling. It must be highlighted, that in all of these studies, only the fuel cell's heat recovery is considered and cooling production is done at the same time that the waste heat is rejected by the fuel cell. In our system we can stored cooling energy without thermal loses. The thermochemical processes enable the storage of energy in the form of chemical potential with no thermal loses.

In this work, a Mixed Integer Linear Programming (MILP) algorithm is used to optimize load demand response and limit the aging of the hydrogen energy system and the battery. The algorithm receives the data of PV production and load consumption over a time horizon and optimize over the same interval. Results can be used as reference for real time operation. The implementation of the algorithm presented in this paper on the real system is planned in the coming months.

The contributions of this paper are to consider thermal recovery of an electrolyzer and a fuel cell for cooling storage, to propose an optimal energy management for a cogeneration system and showing the impact of the TCS on the hydrogen storage system. The paper is organized as follows. The second section gives a brief overview of the system under study. The third section presents the mathematical models for the cogeneration system with the constraints and the objective function of the optimizer. Next, on the fourth section, the results of the energy management over two typical days are presented. Finally, authors summarize the results and discuss about the highlights of this study.

II. System overview

The system is schematized in Fig. 1. It is composed of PV panels, a 48V Li-ion battery, a 0.5Nm^3/h Proton Exchange Membrane (PEM) electrolyzer, a 1 kW PEM fuel cell, a hydrogen tank with 4kg of storage capacity, a heat pump based on a mechanical vapor compression unit used for air conditioning and a thermochemical reactor coupled with the heat pump for cooling storage purposes [11].

Electricity flows from the PV panels to the battery through a DC bus, and to the electrolyzer, the air conditioning unit and the load through an AC bus. The TCS converts the heat from the electrolyzer and the fuel cell into a cooling effect. Finally, the cooling flow from the TCS and from the AC unit is supplied to the thermal load.

The electrical and thermal loads are simulated using the software EnergyPlus. They correspond to the consumption of a hotel room for two people with lights, a refrigerator, a fan, and an AC unit. A more complete description of the system can be found in [6]. For more information on the project readers are invited to visit [12].

III. Modelling

This section first describes the mathematical models of all components from Fig. 1. Then it defines the constraints used into the optimization process and finally presents the objective function. The experimental validation of the electrolyzer and the fuel cell models used in this work can be found in [6].

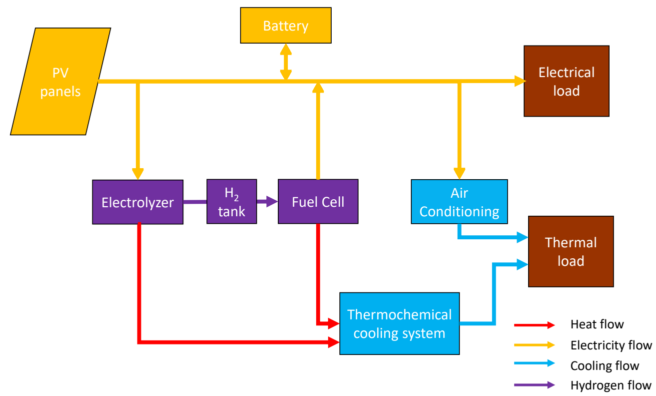

Fig. 1. System overview.

A. Component modelling

The parameters used in the model are summarized in Table I. The Solar radiation was measured near the experimental site in French Polynesia. The PV power available by the solar panels is assumed proportional to the panel area S_{pv} and the yield of the solar panels (converter included) η_{pv}:

$$P_{pv}(t) = \eta_{pv} S_{pv} Irr(t) \tag{1}$$

The actual PV power produced is equal to the available PV power P_{pv} minus the curtailed power P_{curt}, that is the amount of available PV power that is not produced because it cannot be consumed.

The state of charge of the battery (SOC) at the time t is the state of charge at the previous time step minus the energy delivered by the battery P^{dis}_{batt} at the previous time step plus the energy received by the battery P^{ch}_{batt} at the previous time step:

$$SOC(t) = SOC(t-1) + \frac{P^{ch}_{batt}(t-1)\eta_{batt}\Delta t}{Cap_{batt}} - \frac{P^{dich}_{batt}(t-1)\Delta t}{\eta_{batt} Cap_{batt}} \tag{2}$$

η_{batt} is the battery efficiency, Δt is the time step and Cap_{batt} is the battery capacity (in Wh).

The level of hydrogen (LOH) at the time t is the LOH at the previous time step plus the amount of hydrogen supplied by the electrolyzer at the previous time step minus the amount of hydrogen consumed by the fuel cell at the previous time step:

$$LOH(t) = LOH(t-1) + \frac{P_{el}(t-1)\eta_{el}\Delta t}{Cap_{H_2}} - \frac{P_{fc}(t-1)\Delta t}{\eta_{fc} Cap_{H_2}} \tag{3}$$

The electrolyzer efficiency η_{el} is defined by the ratio of hydrogen energy stored and the electrical energy consumed. The fuel cell efficiency η_{fc} is defined by the ratio of the electrical energy produced and the hydrogen energy consumed. P_{el} is the electrical power of the electrolyzer and P_{fc} the electrical power of the fuel cell. Cap_{H_2} is the hydrogen tank capacity (in Wh). It has been computed for a hydrogen tank of 850L at 50 bar.

In order to model the energy storage for cooling production. The term level of cold (LOC) is introduced. This variable measures the amount of liquid ammonia available for cooling production. The LOC at the time t is equal to the LOC at the previous time step plus the amount of thermal energy obtained by the heat recovery of the electrolyzer or the fuel cell at the previous time step minus the cooling production of the TCS at the previous time step:

$$LOC(t) = LOC(t-1) + \frac{Q_i(t-1)COP_{tcs}\Delta t}{Cap_{tcs}} - \frac{Q_{tcs}(t-1)\Delta t}{Cap_{tcs}} \tag{4}$$

Q_{tcs} is the cooling power of the TCS, COP_{tcs} is the coefficient of performance of the thermochemical reactor when recovering heat of the electrolyzer or the fuel cell (Q_i) and Cap_{tcs} is the capacity of the thermochemical reactor, computed as the maximum ammonia mass adsorbed by the reactor multiply by the enthalpy of vaporization of liquid ammonia. The amount of heat produced by the electrolyzer Q_{el} or the fuel cell Q_{fc} is the amount of heat that is produced during the electrochemical reaction assuming that all the heat produced is recoverable:

$$Q_{el}(t) = P_{el}(t)(1-\eta_{el}) \tag{5}$$

$$Q_{fc}(t) = \frac{P_{fc}(t)(1-\eta_{fc})}{\eta_{fc}} \tag{6}$$

The cooling production at the time t $Q_{cool}(t)$ comes from either the TCS or from the heat pump:

$$Q_{cool}(t) = P_{hp}(t)COP_{hp} + Q_{tcs}(t) \tag{7}$$

P_{hp} is the electrical power of the heat pump and COP_{hp} is the coefficient of performance of the heat pump.

TABLE I
MODEL PARAMETERS

S_{pv}	18
η_{pv}	0.20
η_{fc}	0.54
η_{el}	0.67
η_{batt}	0.90
Cap_{batt}	2.2 kWh
Cap_{H_2}	140 kWh
Cap_{tcs}	2.1 kWh
COP_{hp}	4.5
COP_{tcs}	0.46

B. Constraints

The model is subject to the physical constraints of the components. The values of the bounds are presented in Table II.

First of all, the power bounds of each equipment, for instance x is the battery, the fuel cell, the electrolyzer, the heat pump or the cooling power of the thermochemical reactor:

$$P_x^{Min} \leq P_x(t) \leq P_x^{max} \tag{8}$$

In the following, k_x is a binary variable that represents the ON/OFF state of the component x at the time t.

The battery cannot charge and discharge at the same time:

$$k_{batt}^{ch}(t) + k_{batt}^{dis}(t) \leq 1 \tag{9}$$

The fuel cell and the electrolyzer do not work simultaneously:

$$k_{el}(t) + k_{fc}(t) \leq 1 \tag{10}$$

The cooling system cannot produce cooling with the heat pump and with the TCS simultaneously:

$$k_{hp}(t) + k_{tcs}(t) \leq 1 \tag{11}$$

Furthermore, the cooling storage is not possible at the same time that the cooling production:

$$k_{tcs}(t) + k_{fc,el} \leq 1 \tag{12}$$

The upper and lower bounds for the energy storage systems:

$$SOC_{min} \leq SOC(t) \leq SOC_{max} \tag{13}$$

$$LOC_{min} \leq LOC(t) \leq LOC_{max} \tag{14}$$

$$LOH_{min} \leq LOH(t) \leq LOH_{max} \tag{15}$$

To avoid that at the end of the simulation the battery is empty, and in case that several simulations are run consecutively, the final SOC has to be superior or equal to the initial SOC:

$$SOC_{Horizon} \geq SOC_{ini} \tag{16}$$

The power balance of the electrical bus (17) and the limits of the shedding (when the system cannot supply the demand) (18) and curtailment (loss of available PV power) (19):

$$P_{pv}(t) + P_{batt}^{dis}(t) + P_{fc}(t) + P_{ls}(t) = P_{load}(t) + P_{batt}^{ch}(t) + P_{el}(t) + P_{hp}(t) + P_{curt}(t) \tag{17}$$

$$P_{curt}(t) \leq P_{pv}(t) \tag{18}$$

$$P_{ls}(t) \leq P_{load}(t) \tag{19}$$

The power balance of the heat bus (20) and the limits of the curtailment (21) and shedding (22):

$$Q_{cool}(t) + Q_{shed}(t) = Q_{load}(t) + Q_{curt}(t) \tag{20}$$

$$Q_{ls}(t) \leq Q_{load}(t) \tag{21}$$

$$Q_{curt}(t) \leq Q_{cool}(t) \tag{22}$$

TABLE II
CONSTRAINTS BOUNDS

P_{hp}	0.1 - 0.8 kW
P_{fc}	0.3 - 1.5 kW
P_{el}	2.5 - 2.5 kW
P_{batt}	0 - 5 kW
Q_{tcs}	0 -0.6 kW
SOC	0.05 - 1
LOH	0 - 1
LOC	0 - 1

C. Objective function

The objective function is formulated in order to a. reduce the curtailment and shedding power and b. to extend the lifetime of the fuel cell, the electrolyzer and the battery.

To limit the aging of the fuel cell and the electrolyzer, the number of working hours (23) and the number of starts (24) as to be minimized. The number of working hours is defined by:

$$n_x^{hrs}(t) = \sum_{t=1}^{t} k_x(t)\Delta t \tag{23}$$

$\delta k_x(t)$ is defined and represents the state variation of the x-th component. $\delta k_x(t)$ is -1 is for a shutdown, 0 for a hold and 1 for a startup:

$$\delta k_x(t) = k_x(t) - k_x(t-1) \tag{24}$$

The number of cycles for the battery is defined by:

$$n_{batt}^{cyc}(t) = \frac{1}{2}\sum_{t=1}^{t} \frac{P_{batt}^{dis}(t) + P_{batt}^{ch}(t)\Delta t}{Cap_{batt}} \tag{25}$$

The objective function is defined by:

$$\begin{aligned} f = \sum_{t=1}^{Horizon} & c_{ls}P_{ls}(t) + c_{curt}P_{curt}(t) \\ & + c_{ls}Q_{ls}(t) + c_{curt}Q_{curt}(t) \\ & + \frac{C_x^{capex} n_x(t)}{LT_x} + |\delta k_y(t)| \end{aligned} \tag{26}$$

x stands for electrolyzer, fuel cell or battery and y stands for electrolyzer or fuel cell. c is a penalty for PV curtailment, load shedding, cooling curtailment and cooling load shedding. C_{capex} is the capital cost of the electrolyzer, fuel cell or battery. LT stands for the lifetime of the x-th equipment in hours for the fuel cell and the electrolyzer, and in cycles for the battery. The lifetime is defined by the manufacturers. n_x is the number of cycles for the battery and number of hours for the electrolyzer and the fuel cell. The absolute value $|\delta k_y(t)|$ account for the total number of both startups and shutdowns.

D. Evaluation metrics

Metrics are defined in order to compare the studied system with a classical system, without TCS, where there is no heat recovery of the fuel cell and the electrolyzer. The utilization rate of the fuel cell Ur_{fc} is the ratio of electrical energy supplied by the fuel cell $E_{fc}^{supplied}$ and the energy consumed by the load E_{load}^{cons}:

$$Ur_{fc} = \frac{E_{fc}^{supplied}}{E_{load}^{cons}} \tag{27}$$

The utilization rate of the TCS Ur_{tcs} is the ratio of amount of cooling energy provided by the TCS Q_{tcs} and the cooling energy consumed by the load Q_{load} defined by:

$$Ur_{tcs} = \frac{Q_{tcs}}{Q_{load}} \tag{28}$$

The cogeneration efficiency of the fuel cell η_{fc}^{co} is defined by the ratio of the total electrical and cooling energy provided by the amount of hydrogen consumed:

$$\eta_{fc}^{co} = \frac{\sum P_{fc}(t)\Delta t + \sum Q_{fc}(t)COP_{tcs}\Delta t}{\sum \frac{P_{fc}(t)\Delta t}{\eta_{fc}}} \tag{29}$$

The cogeneration efficiency of the electrolyzer η_{el}^{co} is defined by the ratio of the total hydrogen stored plus the cooling energy produced by the amount of electrical energy consumed:

$$\eta_{el}^{co} = \frac{\sum P_{el}(t)\eta_{el}\Delta t + \sum Q_{el}(t)COP_{tcs}\Delta t}{\sum P_{el}(t)\Delta t} \tag{30}$$

IV. Results

Results are presented over two days with a time step of 20 minutes. The problem is formulated in MATLAB and YALMIP [13] language and the solver used is GUROBI.

Fig. 2 describes the electrical power flow and the battery and hydrogen tank state of charge (SOC and LOH). It can be observed that during the day, the PV excess is stored into the battery and transformed into hydrogen by the electrolyzer. And during the night the fuel cell provides the load and the AC unit. During the second day, first the battery is charged until its maximum then, there is an excess of PV power. To avoid PV curtailment, the electrolyzer is turned on, but as the PV power is not sufficient to provide the electrolyzer, the battery is used to complete the power until the battery is almost empty. Then the electrolyzer stops and the battery is charged until its maximum and the electrolyzer in turned on again and like previously, the battery is used to provide enough power to supply the electrolyzer. Then when the battery is empty, the electrolyzer is turned off and the battery charged with the PV excess power.

The Fig. 3 describes the cooling production and consumption on the top and the LOC on the bottom. It can be observed that there is a small part of cooling shedding and curtailment. The continuous operation of the electrolyzer during the first day allows the LOC to return from 0 to 1. During the second day, the electrolyzer and fuel cell's heat recovery refuel the LOC from 0 to 1.

During these two days, the utilization rate of the fuel cell is 73% and the utilization rate of the TCS is 25%. Recovering the heat of the fuel cell for cooling production increased its efficiency from 0.54 to 0.75 and for the electrolyzer from 0.67 to 0.82. Table III shows the impact of the use of the TCS compare to a case of cooling production with a classical

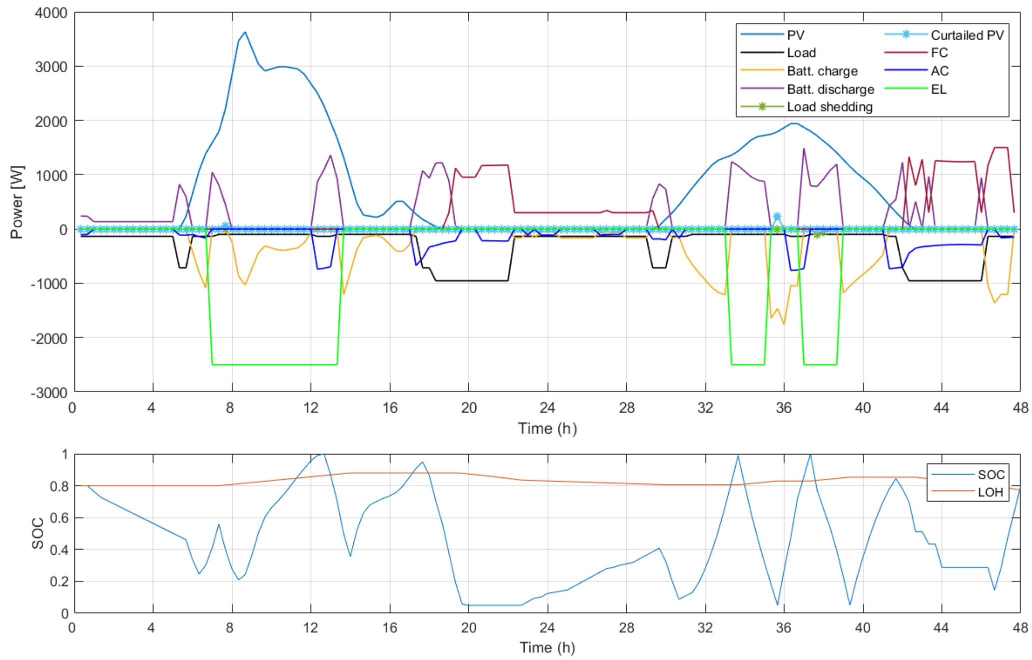

Fig. 2. Power production and consumption (top) and energy level (bottom)

heat pump. As the use of the TCS reduce the electrical consumption, the fuel cell is less used compared to a classical air conditioning. The utilization rate of the fuel cell is reduced by 26% because the electrical consumption is reduced as 25% of the cooling production is made without electrical consumption.

TABLE III
RESULTS

Metrics	With TCS	Classic
Ur_{fc}	0.73	0.96
Ur_{tcs}	0.25	0
η_{el}^{co}	0.82	0.67
η_{fc}^{co}	0.75	0.54

V. Conclusion

In this work, authors have studied a hybrid system for combined cooling and power generation. A MILP algorithm has been used to minimize curtailment and shedding, and limit the system aging. Results showed that the system is able to provide the electrical and thermal needs of the load and the TCS improved the efficiency of the electrolyzer by 15% and of the fuel cell by 21%. In this study, constant efficiency using average values of previous work [6] were considered for the fuel cell, the electrolyzer and the heat pump. In future work, efficiencies will vary according to the operating points of the system's components. To improve the efficiency of the previous component, recovering heat for domestic hot water purpose, in addition to cooling, could be considered.

Acknowledgment

This work has been supported by the French Research Agency under the RECIF project (contract ANR-18-CE05-0043), by the EIPHI Graduate School (contract ANR-17-EURE-0002), and by the Region Bourgogne Franche-Comté. The authors thank Franck Lucas from GEPASUD laboratory for the provision of data used in this work.

References

[1] T. Sylvestre-Baron, *L'Observatoire Polynésien de l'Energie (OPE)*, fr-FR. [Online]. Available: https://www.service-public.pf/sde/lobservatoire-polynesien-des-energies-ope/.

[2] M. Yue, H. Lambert, E. Pahon, R. Roche, S. Jemei, and D. Hissel, "Hydrogen energy systems: A critical review of technologies, applications, trends and challenges," en, *Renewable and Sustainable Energy Reviews*, vol. 146, p. 111 180, Aug. 2021, ISSN: 1364-0321. DOI: 10.1016/j.rser.2021.111180. [Online]. Available: https://www.sciencedirect.com/science/article/pii/S1364032121004688.

[3] H. Lambert, R. Roche, S. Jemei, P. Ortega, and D. Hissel, "Cogénération, trigénération et gestion de l'énergie des systèmes à base de piles à combustible : État de l'art," in *Congrès Français de Thermique*, Belfort, France, Jun. 2020. [Online]. Available: https://hal.archives-ouvertes.fr/hal-02993922.

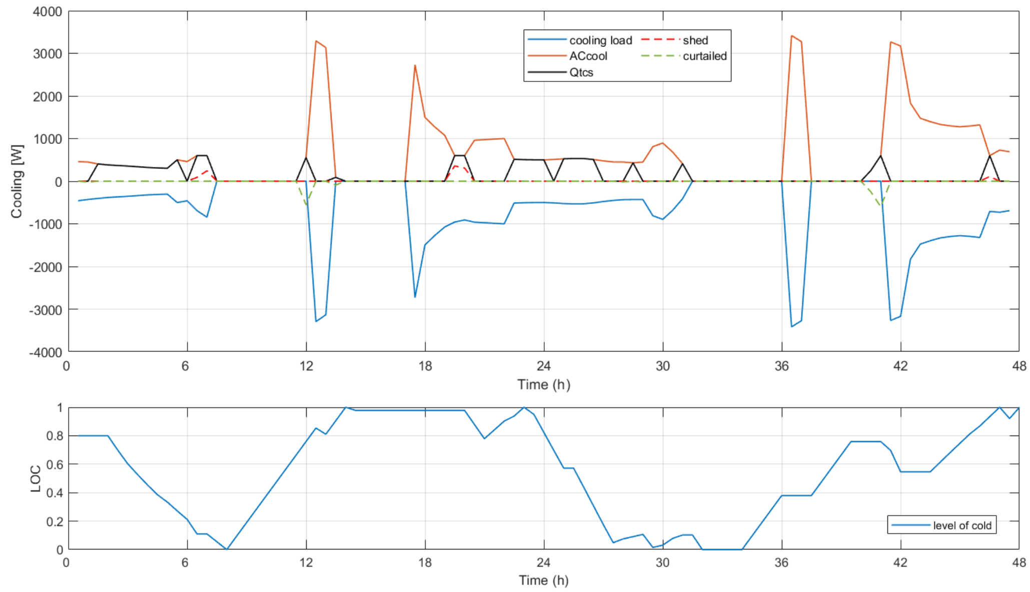

Fig. 3. Cooling production and consumption (top) and level of cold (bottom)

[4] R. Cozzolino, L. Tribioli, and G. Bella, “Power management of a hybrid renewable system for artificial islands: A case study,” en, *Energy*, vol. 106, pp. 774–789, Jul. 2016, ISSN: 0360-5442. DOI: 10.1016/j.energy.2015.12.118. [Online]. Available: https://www.sciencedirect.com/science/article/pii/S0360544215017636.

[5] P. Marocco, D. Ferrero, A. Lanzini, and M. Santarelli, “Optimal design of stand-alone solutions based on RES + hydrogen storage feeding off-grid communities,” en, *Energy Conversion and Management*, vol. 238, p. 114 147, Jun. 2021, ISSN: 0196-8904. DOI: 10.1016/j.enconman.2021.114147. [Online]. Available: https://www.sciencedirect.com/science/article/pii/S019689042100323X.

[6] H. Lambert, R. Roche, S. Jemeï, P. Ortega, and D. Hissel, “Combined Cooling and Power Management Strategy for a Standalone House Using Hydrogen and Solar Energy,” en, *Hydrogen*, vol. 2, no. 2, pp. 207–224, Jun. 2021. DOI: 10.3390/hydrogen2020011. [Online]. Available: https://www.mdpi.com/2673-4141/2/2/11.

[7] H. Q. Nguyen and B. Shabani, “Proton exchange membrane fuel cells heat recovery opportunities for combined heating/cooling and power applications,” en, *Energy Conversion and Management*, p. 112 328, Nov. 2019, ISSN: 0196-8904. DOI: 10.1016/j.enconman.2019.112328. [Online]. Available: http://www.sciencedirect.com/science/article/pii/S0196890419313354.

[8] M. V. Oro, R. G. de Oliveira, and E. Bazzo, “An integrated solution for waste heat recovery from fuel cells applied to adsorption systems,” en, *Applied Thermal Engineering*, vol. 136, pp. 747–754, May 2018, ISSN: 1359-4311. DOI: 10.1016/j.applthermaleng.2018.01.081. [Online]. Available: http://www.sciencedirect.com/science/article/pii/S1359431117351268.

[9] G. Loreti, A. L. Facci, I. Baffo, and S. Ubertini, “Combined heat, cooling, and power systems based on half effect absorption chillers and polymer electrolyte membrane fuel cells,” en, *Applied Energy*, vol. 235, pp. 747–760, Feb. 2019, ISSN: 0306-2619. DOI: 10.1016/j.apenergy.2018.10.109. [Online]. Available: http://www.sciencedirect.com/science/article/pii/S0306261918316805.

[10] A. Perrigot, M. Perier-Muzet, P. Ortega, and D. Stitou, “Technical economic analysis of PV-driven electricity and cold cogeneration systems using particle swarm optimization algorithm,” en, *Energy*, vol. 211, p. 119 009, Nov. 2020, ISSN: 0360-5442. DOI: 10.1016/j.energy.2020.119009. [Online]. Available: http://www.sciencedirect.com/science/article/pii/S0360544220321162.

[11] F. Ferrucci, D. Stitou, P. Ortega, and F. Lucas, “Mechanical compressor-driven thermochemical storage for cooling applications in tropical insular regions. Concept and efficiency analysis,” en, *Applied Energy*, vol. 219, pp. 240–255, Jun. 2018, ISSN: 0306-2619. DOI: 10.1016/j.apenergy.2018.03.049. [Online]. Available: http://www.sciencedirect.com/science/article/pii/S0306261918303787.

[12] *Projet RECIF – Site web du projet RECIF*, en-US. [Online]. Available: https://projetrecif.promes.cnrs.fr/.

[13] J. Löfberg, “Yalmip : A toolbox for modeling and optimization in matlab,” in *In Proceedings of the CACSD Conference*, Taipei, Taiwan, 2004.